Chapter 3

Higher-order stable numerical algorithm for the variable-order time-fractional subdiffusion equation

In this chapter, we have designed a higher-order stable numerical algorithm for the variable-order time-fractional subdiffusion equation by finite difference method. We have applied the newly designed approximation of the variable-order Caputo derivative and a central difference scheme for the spatial derivatives. The full discrete scheme for the problem is constructed, and its matrix representation is given in Sect. 3.2. The theoretical stability of the numerical scheme is discussed in Sect. 3.3. The numerical results and discussion of different cases are covered in Sect. 3.4. The comparative studies are also provided to show the effectiveness and accuracy of numerical scheme. The chapter concludes in Sect. 3.5.

3.1 Introduction

In this paper, we proposed a new numerical approximation for variable order Caputo fractional derivative of order $0 < \alpha(\varkappa, \mathsf{t}) < 1$ by using the idea of interpolation. Later, a numerical scheme is presented by using finite difference approach for variable order time fractional sub-diffusion equation (VOTFSDE).

3.1.1 Formulation of the problem

Consider the following variable-order time-fractional subdiffusion equation (VOTFSDE) [64]:

$$\frac{\partial \mathrm{u}(r,\mathsf{t})}{\partial \mathsf{t}} = {}_{RL}D_{0,\mathsf{t}}^{1-\alpha(r,\mathsf{t})}\left[\frac{\partial^2 \mathrm{u}(r,\mathsf{t})}{\partial r^2}\right] + \mathsf{f}(r,\mathsf{t}) \tag{3.1}$$

with initial condition

$$\mathrm{u}(r,0) = \Phi(r), \tag{3.2}$$

and the Dirichlet boundary condition

$$\mathrm{u}(0,\mathsf{t}) = \Psi_1(\mathsf{t}),\ \mathrm{u}(\mathrm{L},\mathsf{t}) = \Psi_2(\mathsf{t}). \tag{3.3}$$

For the function $\mathsf{f}(r,\mathsf{t})$, the Riemann-Liouville integration of order $\alpha(r,\mathsf{t}) > 0$ is given as [13]

$${}_{RL}D_{a,\mathsf{t}}^{-\alpha(r,\mathsf{t})}\mathsf{f}(r,\mathsf{t}) = \frac{1}{\Gamma\alpha(r,\mathsf{t})}\int_a^{\mathsf{t}} (\mathsf{t}-s)^{\alpha(r,\mathsf{t})-1}\mathsf{f}(r,s)ds. \tag{3.4}$$

Applying Riemann-Liouville integration in time in (3.1), we obtain

$$ {}_{RL}D_{0,\mathsf{t}}^{-(1-\alpha(r,\mathsf{t}))}\frac{\partial \mathsf{u}(r,\mathsf{t})}{\partial \mathsf{t}} = \frac{\partial^2 \mathsf{u}(r,\mathsf{t})}{\partial \mathsf{t}^2} + {}_{RL}D_{0,\mathsf{t}}^{-(1-\alpha(r,\mathsf{t}))}\mathsf{f}(r,\mathsf{t}). \tag{3.5} $$

Now, using the property

$$ {}_{RL}D_{a,\mathsf{t}}^{-\alpha(r,\mathsf{t})}\left({}_{RL}D_{a,\mathsf{t}}^{\alpha(r,\mathsf{t})}\right) = \mathsf{f}(r,\mathsf{t}) - \sum_{\mathrm{j}=1}^{n}\left[{}_{RL}D_{a,\mathsf{t}}^{(\alpha(r,\mathsf{t})-\mathrm{j})}\mathsf{f}(r,\mathsf{t})\right]_{\mathsf{t}=a}\frac{(\mathsf{t}-a)^{\alpha(r,\mathsf{t})-\mathrm{j}}}{\Gamma(\alpha(r,\mathsf{t})-\mathrm{j}+1)}. \tag{3.6} $$

Here, $(n-1) < \alpha(r,\mathsf{t}) < n$. For the function $\mathsf{f}(r,\mathsf{t})$, the relationship between the Caputo and Riemann-Liouville derivative is given by [13]

$$ {}_{RL}D_{a,\mathsf{t}}^{\alpha(r,\mathsf{t})}\mathsf{f}(r,\mathsf{t}) = {}_{C}D_{a,\mathsf{t}}^{\alpha(r,\mathsf{t})}\mathsf{f}(r,\mathsf{t}) + \sum_{\mathrm{z}=0}^{n-1}\frac{1}{\Gamma(\mathrm{z}+1-\alpha(r,\mathsf{t}))}\mathsf{f}^{\mathrm{z}}(r,a)(\mathsf{t}-a)^{\mathrm{z}-\alpha(r,\mathsf{t})}. \tag{3.7} $$

For $n = 1$, The form of the relationship is

$$ {}_{RL}D_{a,\mathsf{t}}^{\alpha(r,\mathsf{t})}\mathsf{f}(r,\mathsf{t}) = {}_{C}D_{a,\mathsf{t}}^{\alpha(r,\mathsf{t})}\mathsf{f}(r,\mathsf{t}) + \frac{1}{\Gamma(1-\alpha(r,\mathsf{t}))}\mathsf{f}(r,a)(\mathsf{t}-a)^{-\alpha(r,\mathsf{t})}. \tag{3.8} $$

After using the relation (3.8) and (3.6) in eqn. (3.5), we obtain

$$ {}_{C}D_{0,\mathsf{t}}^{\alpha(r,\mathsf{t})}\mathrm{u}(r,\mathsf{t}) = \frac{\partial^2 \mathrm{u}(r,\mathsf{t})}{\partial r^2} + {}_{RL}D_{0,\mathsf{t}}^{-(1-\alpha(r,\mathsf{t}))}\mathsf{f}(r,\mathsf{t}). \tag{3.9} $$

Hence, the problem (3.1) has been transformed to the following VOTFSDE

$$ {}_{C}D_{0,\mathsf{t}}^{\alpha(r,\mathsf{t})}\mathrm{u}(r,\mathsf{t}) = \frac{\partial^2 \mathrm{u}(r,\mathsf{t})}{\partial r^2} + \mathrm{g}(r,\mathsf{t}) \tag{3.10} $$

with initial and Dirichlet boundary conditions

$$ \mathrm{u}(r,0) = \Phi(r), \tag{3.11} $$

$$ \mathrm{u}(0,\mathsf{t}) = \Psi_1(\mathsf{t}),\ \mathrm{u}(\mathrm{L},\mathsf{t}) = \Psi_2(\mathsf{t}). \tag{3.12} $$

where

$$\mathrm{g}(r,\mathrm{t}) = {}_{RL}D_{0,\mathrm{t}}^{-(1-\alpha(r,\mathrm{t}))}\mathrm{f}(r,\mathrm{t}) = \frac{1}{\Gamma(1-\alpha(r,\mathrm{t}))}\int_0^{\mathrm{t}} \frac{\mathrm{f}(r,\eta)}{(\mathrm{t}-\eta)^{\alpha(r,\mathrm{t})}}d\eta.$$

Here ${}_{C}D_{0,\mathrm{t}}^{\alpha(r,\mathrm{t})}$ denotes the VO Caputo type differential operator of order $\alpha(r,\mathrm{t})$, where $(0<\alpha(r,\mathrm{t})<1)$. The VOCD is defined as

$${}_{C}D_{0,\mathrm{t}}^{\alpha(r,\mathrm{t})}\mathrm{u}(r,\mathrm{t}) = \begin{cases} \dfrac{1}{\Gamma(n-\alpha(r,\mathrm{t}))}\int_0^{\mathrm{t}}(\mathrm{t}-s)^{n-\alpha(r,\mathrm{t})-1}\mathrm{u}^n(r,s)ds, & n-1<\alpha(r,\mathrm{t})<n, \\ \mathrm{u}^n(r,\mathrm{t}), \quad \alpha(r,\eta)=n\in\mathbf{N}. \end{cases} \tag{3.13}$$

The main contribution of this chapter are given below.

- We have used the L-123 approximation [188] of the VOCD of order $(0<\alpha(r,\mathrm{t})<1)$.
- A difference scheme is designed for solving variable-order time-fractional subdiffusion equation. The scheme has been proven to be completely stable.
- Computational algorithm is also provided for a better understanding of proposed numerical scheme.
- Three numerical examples are tested to validate the proposed numerical method. Precise and higher order of convergence can be shown in numerical results.
- A comparative studies with [1, 35] are also provided to show the accuracy and effectiveness of the proposed numerical scheme.

3.1.2 L-123 approximation for the variable-order Caputo derivative

The L-123 approximation for the variable-order Caputo fractional derivative of order $\alpha(r,\mathsf{t}) \in (0,1)$ is provided in [188]. Let $\tilde{\mathbb{D}}_{\mathsf{t}}^{\alpha(r_\mathsf{i},\mathsf{t}_\mathsf{z})}$ be the approximation of the variable-order Caputo derivative ${}_0^C D_{\mathsf{t}}^{\alpha(r_\mathsf{i},\mathsf{t}_\mathsf{z})}\mathsf{f}(r,\mathsf{t})$, therefore,

$$\tilde{\mathbb{D}}_{\mathsf{t}}^{\alpha(r_\mathsf{i},\mathsf{t}_\mathsf{z})}\mathsf{f}(r,\mathsf{t})\Big|_{\mathsf{t}=\mathsf{t}_\mathsf{z}} = \frac{\tau^{1-\alpha(r_\mathsf{i},\mathsf{t}_\mathsf{z})}}{\Gamma(2-\alpha(r_\mathsf{i},\mathsf{t}_\mathsf{z}))}\Bigg(\sum_{\mathsf{j}=1}^{\mathsf{z}} a_{\mathsf{z}-\mathsf{j}}^{(r_\mathsf{i},\mathsf{t}_\mathsf{z})}\delta_\mathsf{t}\mathsf{f}(r_\mathsf{i},\mathsf{t}_{\mathsf{j}-\frac{1}{2}}) + \sum_{\mathsf{j}=2}^{\mathsf{z}} b_{\mathsf{z}-\mathsf{j}}^{\alpha(r_\mathsf{i},\mathsf{t}_\mathsf{z})}(\delta_\mathsf{t}\mathsf{f}(r_\mathsf{i},\mathsf{t}_{\mathsf{j}-\frac{1}{2}}) - \delta_\mathsf{t}\mathsf{f}(r_\mathsf{i},\mathsf{t}_{\mathsf{j}-\frac{3}{2}})) + \sum_{\mathsf{j}=3}^{\mathsf{z}} \beta_{\mathsf{z}-\mathsf{j}}^{\alpha(r_\mathsf{i},\mathsf{t}_\mathsf{z})}(\delta_\mathsf{t}\mathsf{f}(r_\mathsf{i},\mathsf{t}_{\mathsf{j}-\frac{1}{2}}) - 2\delta_\mathsf{t}\mathsf{f}(r_\mathsf{i},\mathsf{t}_{\mathsf{j}-\frac{3}{2}}) + \delta_\mathsf{t}\mathsf{f}(r_\mathsf{i},\mathsf{t}_{\mathsf{j}-\frac{5}{2}}))\Bigg) \tag{3.14}$$

$$= \frac{\tau^{1-\alpha(r_\mathsf{i},\mathsf{t}_\mathsf{z})}}{\Gamma(2-\alpha(r_\mathsf{i},\mathsf{t}_\mathsf{z}))}\sum_{\mathsf{j}=1}^{k} \Upsilon_{\mathsf{z}-\mathsf{j}}^{\alpha(r_\mathsf{i},\mathsf{t}_\mathsf{z})}\delta_\mathsf{t}\mathsf{f}(r_\mathsf{i},\mathsf{t}_{\mathsf{j}-\frac{1}{2}}) \tag{3.15}$$

$$= \frac{\tau^{-\alpha(r_\mathsf{i},\mathsf{t}_\mathsf{z})}}{\Gamma(2-\alpha(r_\mathsf{i},\mathsf{t}_\mathsf{z}))}\Bigg(\Upsilon_0^{\alpha(r_\mathsf{i},\mathsf{t}_\mathsf{z})}\mathsf{f}(r_\mathsf{i},\mathsf{t}_\mathsf{z}) - \sum_{\mathsf{j}=1}^{k-1}(\Upsilon_{\mathsf{z}-\mathsf{j}-1}^{\alpha(r_\mathsf{i},\mathsf{t}_\mathsf{z})} - \Upsilon_{\mathsf{z}-\mathsf{j}}^{\alpha(r_\mathsf{i},\mathsf{t}_\mathsf{z})})\mathsf{f}(r_\mathsf{i},\mathsf{t}_\mathsf{j}) - \Upsilon_{\mathsf{z}-1}^{\alpha(r_\mathsf{i},\mathsf{t}_\mathsf{z})}\mathsf{f}(r_\mathsf{i},\mathsf{t}_0)\Bigg) \tag{3.16}$$

Lemma 3.1.1 ([188]). For any $\alpha(r_\mathsf{i},\mathsf{t}_\mathsf{z})$ $(0 < \alpha(r_\mathsf{i},\mathsf{t}_\mathsf{z}) < 1)$, we have

- $\beta_\mathsf{j}^{(\alpha(r_\mathsf{i},\mathsf{t}_\mathsf{z}))} \geq 0,\ \mathsf{j} \leq 0;$
- $\beta_\mathsf{j}^{(\alpha(r_\mathsf{i},\mathsf{t}_\mathsf{z}))}$ decreases strictly monotonically for $\mathsf{j} = 0,1,2\ldots\mathsf{z}-1.$

Lemma 3.1.2 ([188]). For any $\alpha(r_\mathsf{i},\mathsf{t}_\mathsf{z})$ $(0 < \alpha(r_\mathsf{i},\mathsf{t}_\mathsf{z}) < 1)$, and $\Upsilon_\mathsf{j}^{(\alpha(r_\mathsf{i},\mathsf{t}_\mathsf{z}))}$ $(0 \leq \mathsf{j} \leq \mathsf{z}-1, \mathsf{z} \geq 4)$ defined, it holds

1. $\Upsilon_0^{(\alpha(r_\mathsf{i},\mathsf{t}_\mathsf{z}))} \geq |\Upsilon_1^{(\alpha(r_\mathsf{i},\mathsf{t}_\mathsf{z}))}|;$
2. $\Upsilon_\mathsf{j}^{(\alpha(r_\mathsf{i},\mathsf{t}_\mathsf{z}))} > 0,\ \mathsf{j} \neq 1;$
3. $\Upsilon_2^{(\alpha(r_\mathsf{i},\mathsf{t}_\mathsf{z}))} \geq \Upsilon_3^{(\alpha(r_\mathsf{i},\mathsf{t}_\mathsf{z}))} \geq \cdots \geq \Upsilon_{\mathsf{z}-1}^{(\alpha(r_\mathsf{i},\mathsf{t}_\mathsf{z}))};$

4. $\Upsilon_0^{(\alpha(r_i,t_z))} > \Upsilon_2^{(\alpha(r_i,t_z))}$;

5. $\sum_{j=0}^{z-1} \Upsilon_0^{(\alpha(r_i,t_z))} = z^{(1-\alpha(r_i,t_z))}$.

Proof. The proof follows [185]. □

Theorem 3.1.1. Suppose $f(r,t) \in C_{r,t}^{2,4}([0,L]\times[0,t_z])$. For any $\alpha(r_i,t_z)$, $\tilde{\mathbb{D}}_t^{\alpha(r_i,t_z)} f(r,t)|_{t=t_z}$ is defined in (3.14). $R(f(r_i,t_z))$ is showing the truncation error, $|R(f(r_i,t_z))|$ $= {}_0^C D_t^{\alpha(r_i,t_z)} f(r,t)|_{t=t_z} - \tilde{\mathbb{D}}_t^{\alpha(r_i,t_z)} f(r,t)|_{t=t_z}$. Then we get

$$|R(f(r_i,t_1))| \leq \frac{\alpha(r_i,t_z)}{2\Gamma(3-\alpha(r_i,t_z))}\Delta t^{2-\{\alpha(r_i,t_z)} \max_{t_0\leq t\leq t_1} f''(t), \tag{3.17}$$

$$\begin{aligned}|R(f(r_i,t_2))| \leq \frac{\alpha(r_i,t_z)}{\Gamma(1-\alpha(r_i,t_z))}\Bigg(&\frac{1}{12}\max_{t_0\leq t\leq t_1}|f''(t)|(t_2-t_1)^{-\alpha(r_i,t_z)-1}\Delta t^3 \\ &+\frac{1}{3(1-\alpha(r_i,t_z))(2-\alpha(r_i,t_z))}\left(\frac{1}{2}+\frac{1}{3-\alpha(r_i,t_z)}\right)\max_{t_0\leq t\leq t_2}|f'''(t)|\Delta t^{3-\alpha(r_i,t_z)}\Bigg),\end{aligned} \tag{3.18}$$

$$\begin{aligned}|R(f(r_i,t_z))| \leq \frac{\alpha(r_i,t_z)}{\Gamma(1-\alpha(r_i,t_z))}\Bigg(&12(t_z-t_1)^{-\alpha(r_i,t_z)-1}\max_{t_0\leq t\leq t_1}|f''(t)|\Delta t^3+\frac{1}{8}(t_z-t_2)^{-\alpha(r_i,t_z)-1} \\ &\max_{t_0\leq t\leq t_2}|f'''(t)|\Delta t^4+\left(\frac{1}{2}+\frac{1}{12}\frac{27-10\alpha(r_i,t_z)+\alpha(r_i,t_z)^2}{\mathcal{P}_{i=1}^4(\alpha(r_i,t_z)i)}\right) \\ &\max_{t_0\leq t\leq t_z}|f^4(t)|\Delta t^{4-\alpha(r_i,t_z)}\Bigg),\ z\geq 3.\end{aligned} \tag{3.19}$$

Proof. Similar described in [185]. □

3.2 Numerical algorithm for the variable-order time-fractional subdiffusion equation (VOTFSDE)

We have suppose the domain $\mho(r,\mathrm{t}) = [0,\mathrm{L}]\times[0,\mathrm{T}]$. Let's suppose $h = \mathrm{L}/\mathbf{M}$ and $\tau = \mathrm{T}/\mathbf{N}$, where $\mathbf{M}$ and $\mathbf{N}$ be the number of grid points in both space and time, respectively. $r_{\mathrm{i}} = \mathrm{i}h, \mathrm{i} = 0,1\ldots\mathbf{M}$ and $\mathrm{t}_{\mathrm{z}} = \mathrm{z}\tau,\ \mathrm{z} = 0,1\ldots\mathbf{N}$. Where r_{i} and t_{z} stand for space and time grid points.

The VOTFSDE at the any grid point $(r_{\mathrm{i}},\mathrm{t}_{\mathrm{z}})$ can be expressed as:

$$ {}_{0}^{C}D_{\mathrm{t}}^{\alpha(r_{\mathrm{i}},\mathrm{t}_{\mathrm{z}})}\mathrm{f}(r,\mathrm{t})|_{\mathrm{t}=\mathrm{t}_{\mathrm{z}}} = \frac{\partial^2 \mathrm{u}(r_{\mathrm{i}},\mathrm{t}_{\mathrm{z}})}{\partial r^2} + \mathrm{g}_{\mathrm{i}}^{\mathrm{z}}, \tag{3.20} $$

where boundaries are $\mathrm{u}_{\mathrm{i}}^{0} = \Phi(r_{\mathrm{i}}), \mathrm{i} = 0,1,2\ldots\mathbf{M}$; $\mathrm{u}_{0}^{\mathrm{z}} = \Psi_1(\mathrm{t}_{\mathrm{z}})$; $\mathrm{u}_{\mathbf{M}}^{\mathrm{z}} = \Psi_2(\mathrm{t}_{\mathrm{z}})$, $\mathrm{z} = 1,2,\ldots\mathbf{N}$, and $\mathrm{g}_{\mathrm{i}}^{\mathrm{z}} = \mathrm{g}(r_{\mathrm{i}},\mathrm{t}_{\mathrm{z}})$. The central difference approximation for the second order spatial derivative is given by

$$ \frac{\partial^2 \mathrm{u}(r_{\mathrm{i}},\mathrm{t}_{\mathrm{z}})}{\partial r^2} = \frac{\mathrm{u}(r_{i+1},\mathrm{t}_{\mathrm{z}}) - 2\mathrm{u}(r_{\mathrm{i}},\mathrm{t}_{\mathrm{z}}) + \mathrm{u}(r_{i-1},\mathrm{t}_{\mathrm{z}})}{h^2} + O(h^2). \tag{3.21} $$

Here we are using the suggested L-123 approximation (3.15) for the VOCD in (3.20).

$$ \frac{\tau^{-\alpha(r_{\mathrm{i}},\mathrm{t}_{\mathrm{z}})}}{\Gamma(2-\alpha(r_{\mathrm{i}},\mathrm{t}_{\mathrm{z}}))}\sum_{\mathrm{j}=0}^{\mathrm{z}-1}\Upsilon_{i,\mathrm{z}-\mathrm{j}}^{\alpha(r_{\mathrm{i}},\mathrm{t}_{\mathrm{z}})}[\mathrm{u}_{\mathrm{i}}^{\mathrm{j}+1} - \mathrm{u}_{\mathrm{i}}^{\mathrm{j}}] = \frac{\mathrm{u}_{i+1}^{\mathrm{z}} - 2\mathrm{u}_{\mathrm{i}}^{\mathrm{z}} + \mathrm{u}_{i-1}^{\mathrm{z}}}{h^2} + \mathrm{g}_{\mathrm{i}}^{\mathrm{z}} \tag{3.22} $$

$$ \frac{\tau^{-\alpha(r_{\mathrm{i}},\mathrm{t}_{\mathrm{z}})}}{\Gamma(2-\alpha(r_{\mathrm{i}},\mathrm{t}_{\mathrm{z}}))}\left[\Upsilon_{0}^{\alpha(r_{\mathrm{i}},\mathrm{t}_{\mathrm{z}})}u_{\mathrm{i}}^{\mathrm{z}} - \sum_{\mathrm{j}=1}^{\mathrm{z}-1}(\Upsilon_{\mathrm{z}-\mathrm{j}-1}^{\alpha(r_{\mathrm{i}},\mathrm{t}_{\mathrm{z}})} - \Upsilon_{\mathrm{z}-\mathrm{j}}^{\alpha(r_{\mathrm{i}},\mathrm{t}_{\mathrm{z}})})u_{\mathrm{i}}^{\mathrm{j}} - \Upsilon_{\mathrm{z}-1}^{\alpha(r_{\mathrm{i}},\mathrm{t}_{\mathrm{z}})}u_{\mathrm{i}}^{0}\right] = \frac{\mathrm{u}_{i+1}^{\mathrm{z}} - 2\mathrm{u}_{\mathrm{i}}^{\mathrm{z}} + \mathrm{u}_{i-1}^{\mathrm{z}}}{h^2} + \mathrm{g}_{\mathrm{i}}^{\mathrm{z}} \tag{3.23} $$

$$\mathrm{u}_{\mathrm{i}}^{\mathrm{z}}-\frac{1}{\Upsilon_0^{\alpha(r_{\mathrm{i}},\mathrm{t_z})}}\left[\sum_{\mathrm{j}=1}^{\mathrm{z}-1}\left(\Upsilon_{\mathrm{z-j}-1}^{\alpha(r_{\mathrm{i}},\mathrm{t_z})}-\Upsilon_{\mathrm{z-j}}^{\alpha(r_{\mathrm{i}},\mathrm{t_z})}\right)\mathrm{u}_{\mathrm{i}}^{\mathrm{j}}+\Upsilon_{\mathrm{z}-1}^{\alpha(r_{\mathrm{i}},\mathrm{t_z})}\mathrm{u}_{\mathrm{i}}^{o}\right]=\mu(r_{\mathrm{i}},\mathrm{t_z})\frac{\left(\mathrm{u}_{i+1}^{\mathrm{z}}-2\mathrm{u}_{\mathrm{i}}^{\mathrm{z}}+\mathrm{u}_{i-1}^{\mathrm{z}}\right)}{h^2}$$
$$+\mu(r_{\mathrm{i}},\mathrm{t_z})\mathrm{g}_{\mathrm{i}}^{\mathrm{z}}. \tag{3.24}$$

Here, $\mu(r_{\mathrm{i}},\mathrm{t_z})=\dfrac{\Gamma(2-\alpha(r_{\mathrm{i}},\mathrm{t_z}))}{\tau^{-\alpha(r_{\mathrm{i}},\mathrm{t_z})}\Upsilon_0^{\alpha(r_{\mathrm{i}},\mathrm{t_z})}}$. Then the designed scheme 3.24 can be written as,

$$\mathrm{u}_{\mathrm{i}}^{\mathrm{z}}-\mu(r_{\mathrm{i}},\mathrm{t_z})\frac{\left(\mathrm{u}_{i+1}^{\mathrm{z}}-2\mathrm{u}_{\mathrm{i}}^{\mathrm{z}}+\mathrm{u}_{i-1}^{\mathrm{z}}\right)}{h^2}=\frac{1}{\Upsilon_0^{\alpha(r_{\mathrm{i}},\mathrm{t_z})}}\left[\sum_{\mathrm{j}=1}^{\mathrm{z}-1}\left(\Upsilon_{\mathrm{z-j}-1}^{\alpha(r_{\mathrm{i}},\mathrm{t_z})}-\Upsilon_{\mathrm{z-j}}^{\alpha(r_{\mathrm{i}},\mathrm{t_z})}\right)u_{\mathrm{i}}^{\mathrm{j}}+\Upsilon_{\mathrm{z}-1}^{\alpha(r_{\mathrm{i}},\mathrm{t_z})}u_{\mathrm{i}}^{o}\right]$$
$$+\mu(r_{\mathrm{i}},\mathrm{t_z})\mathrm{g}_{\mathrm{i}}^{\mathrm{z}}. \tag{3.25}$$

The matrix form of above equation (3.25), we obtain

$$\mathrm{U}^{k}+\mathbb{B}\mathbb{E}\mathrm{U}^{\mathrm{z}}=\frac{1}{\Upsilon_0^{\alpha(r_{\mathrm{i}},\mathrm{t_z})}}\left[\sum_{\mathrm{j}=1}^{\mathrm{z}-1}\left(\Upsilon_{\mathrm{z-j}-1}^{\alpha(r_{\mathrm{i}},\mathrm{t_z})}-\Upsilon_{\mathrm{z-j}}^{\alpha(r_{\mathrm{i}},\mathrm{t_z})}\right)\mathrm{U}^{\mathrm{j}}+\Upsilon_{\mathrm{z}-1}^{\alpha(r_{\mathrm{i}},\mathrm{t_z})}\mathrm{U}^{0}\right]+\mathbb{B}\mathrm{G}^{\mathrm{z}}. \tag{3.26}$$

Where $\mathrm{U_z}=[\mathrm{u}_1^{\mathrm{z}},\mathrm{u}_2^{\mathrm{z}},\ldots,\mathrm{u}_{M-1}^{\mathrm{z}}]^{\mathrm{T}}$ and $\mathcal{G}_{\mathrm{z}}=[\mathrm{g}_1^{\mathrm{z}},\mathrm{g}_2^{\mathrm{z}},\ldots,\mathrm{g}_{M-1}^{\mathrm{z}}]^{\mathrm{T}}$.

$$\mathbb{B}=\begin{bmatrix}\mu(r_1,\mathrm{t_z}) & 0 & \ldots & 0\\ 0 & \mu(r_2,\mathrm{t_z}) & \ldots & 0\\ \vdots & \vdots & \ddots & \vdots\\ 0 & 0 & \ldots & \mu(r_{\mathbf{M}-1},\mathrm{t_z})\end{bmatrix}_{\mathbf{M}-1\times\mathbf{M}-1}. \tag{3.27}$$

$$\mathbb{E}=\frac{1}{h^2}\begin{bmatrix}2 & -1 & 0 & \ldots & 0\\ -1 & 2 & -1 & \ldots & 0\\ 0 & -1 & 2 & \ldots & 0\\ \vdots & \vdots & \vdots & \ddots & \vdots\\ 0 & 0 & 0 & \ldots & 2\end{bmatrix}_{\mathbf{M}-1\times\mathbf{M}-1}. \tag{3.28}$$

3.3 Stability of the numerical scheme

Theorem 3.3.1. The error estimation of the proposed scheme is

$$\|\zeta^{\mathrm{z}}\|_2 \leq \|\zeta^0\|_0. \tag{3.29}$$

This proves the stability of our scheme.

Proof. Suppose $\mathrm{U}_{\mathrm{i}}^n$ and $\bar{\mathrm{u}}_{\mathrm{i}}^n$ be the approximate and the exact solution of numerical scheme. The error is is showinged by $\zeta_{\mathrm{i}}^k = \bar{\mathrm{u}}_{\mathrm{i}}^{\mathrm{z}} - \mathrm{U}_{\mathrm{i}}^{\mathrm{z}}$. The difference scheme (3.26) will also be satisfied by this error

$$\zeta^{\mathrm{z}} + \mathbb{B}\mathbb{E}\zeta^{\mathrm{z}} = \frac{1}{\Upsilon_0^{\alpha(r_{\mathrm{i}},\mathrm{t_z})}} \left[\sum_{\mathrm{j}=1}^{\mathrm{z}-1} \left(\Upsilon_{\mathrm{z-j-1}}^{\alpha(r_{\mathrm{i}},\mathrm{t_z})} - \Upsilon_{\mathrm{z-j}}^{\alpha(r_{\mathrm{i}},\mathrm{t_z})} \right) \zeta^{\mathrm{j}} + \Upsilon_{\mathrm{z}-1}^{\alpha(r_{\mathrm{i}},\mathrm{t_z})} \zeta^0 \right]. \tag{3.30}$$

Since $\mathbb{H}$ is an orthogonal matrix such that $\mathbb{E}$ is a symmetric matrix.

$$\mathbb{E} = \mathbb{H}^T A \mathbb{H}, \tag{3.31}$$

where $A = diag(\lambda_1, \lambda_2, \cdots, \lambda_{M-1})$ is a diagonal matrix with eigen values of $\mathbb{E}$ and $\mathbb{H}^T$is the transposed version of matrix $\mathbb{H}$. After left multiplication of both side of (3.30) by $\mathbb{H}$ and Using (3.31) we get,

$$\mathbb{H}\zeta^{\mathrm{z}} + \mathbb{B}\mathbb{H}\mathbb{H}^T A \mathbb{H}\zeta^{\mathrm{z}} = \frac{1}{\Upsilon_0^{\alpha(r_{\mathrm{i}},\mathrm{t_z})}} \left[\sum_{\mathrm{j}=1}^{\mathrm{z}-1} \left(\Upsilon_{\mathrm{z-j-1}}^{\alpha(r_{\mathrm{i}},\mathrm{t_z})} - \Upsilon_{\mathrm{z-j}}^{\alpha(r_{\mathrm{i}},\mathrm{t_z})} \right) \mathbb{H}\zeta^{\mathrm{j}} + \Upsilon_{\mathrm{z}-1}^{\alpha(r_{\mathrm{i}},\mathrm{t_z})} \mathbb{H}\zeta^0 \right]. \tag{3.32}$$

Let $\mathbb{H}\zeta^{\mathrm{z}} = \bar{\zeta}^{\mathrm{z}}$, then the above equation becomes

$$\bar{\zeta}^{\mathrm{z}} + \mathbb{B}A\bar{\zeta}^{\mathrm{z}} = \frac{1}{\Upsilon_0^{\alpha(r_{\mathrm{i}},\mathrm{t_z})}} \left[\sum_{\mathrm{j}=1}^{\mathrm{z}-1} \left(\Upsilon_{\mathrm{z-j-1}}^{\alpha(r_{\mathrm{i}},\mathrm{t_z})} - \Upsilon_{\mathrm{z-j}}^{\alpha(r_{\mathrm{i}},\mathrm{t_z})} \right) \bar{\zeta}^{\mathrm{j}} + \Upsilon_{\mathrm{z}-1}^{\alpha(r_{\mathrm{i}},\mathrm{t_z})} \bar{\zeta}^0 \right]. \tag{3.33}$$

Since $\mathbb{H}$ is orthogonal matrix it follows that $\|\zeta^{z}\|_2 = \|\bar{\zeta}^{z}\|_2$, then the theorem will be proved if we show that

$$\|\bar{\zeta}^{z}\|_2 \leq \|\bar{\zeta}^{0}\|_0, \tag{3.34}$$

for every $\mathsf{i}, \mathsf{i} = 1, 2, \ldots, \mathbf{M} - 1$ in (3.32), we have

$$(1 + \mu(r_{\mathsf{i}}, \mathsf{t}_{z})\lambda_{\mathsf{i}})\,\bar{\zeta}^{z} = \frac{1}{\Upsilon_{0}^{\alpha(r_{\mathsf{i}},\mathsf{t}_{z})}}\left[\sum_{\mathsf{j}=1}^{z-1}\left(\Upsilon_{z-\mathsf{j}-1}^{\alpha(r_{\mathsf{i}},\mathsf{t}_{z})} - \Upsilon_{z-\mathsf{j}}^{\alpha(r_{\mathsf{i}},\mathsf{t}_{z})}\right)\bar{\zeta}^{\mathsf{j}} + \Upsilon_{z-1}^{\alpha(r_{\mathsf{i}},\mathsf{t}_{z})}\bar{\zeta}^{0}\right]. \tag{3.35}$$

We now demonstrate from (3.35) that the following inequality holds for each occurence of $\mathsf{i}, \mathsf{i} = 1, 2, \ldots, \mathbf{M} - 1$,

$$|\bar{\zeta}_{\mathsf{i}}^{z}| \leq |\bar{\zeta}_{\mathsf{i}}^{0}|. \tag{3.36}$$

Clearly for $z = 1$, we have

$$(1 + \mu(r_{\mathsf{i}}, \mathsf{t}_{1})\lambda_{\mathsf{i}})\,\bar{\zeta}^{1} = \bar{\zeta}^{0}. \tag{3.37}$$

$$|\bar{\zeta}^{1}| = \frac{1}{|1 + \mu(r_{\mathsf{i}}, \mathsf{t}_{1})\lambda_{\mathsf{i}}|}|\bar{\zeta}^{0}|, \tag{3.38}$$

we have

$$\frac{1}{|1 + \mu(r_{\mathsf{i}}, \mathsf{t}_{1})\lambda_{\mathsf{i}}|} \leq 1. \tag{3.39}$$

$$|\bar{\zeta}_{\mathsf{j}}^{1}| \leq |\bar{\zeta}_{\mathsf{j}}^{0}|. \tag{3.40}$$

Now, assume that the inequality given below holds for $\mathsf{j} = 0, 1, 2, \ldots, z - 1$.

$$|\bar{\zeta}_{\mathsf{i}}^{\mathsf{j}}| \leq |\bar{\zeta}_{\mathsf{i}}^{0}|. \tag{3.41}$$

Therefore, we reach the following conclusion for $\mathrm{j} = \mathrm{z}$ through mathematical induction.

$$|\bar{\zeta}^{\mathrm{z}}| = \frac{1}{(1+\mu(r_{\mathrm{i}},\mathrm{t}_{\mathrm{z}})\lambda_{\mathrm{i}})\,\Upsilon_0^{\alpha(r_{\mathrm{i}},\mathrm{t}_{\mathrm{z}})}} \left| \sum_{\mathrm{j}=1}^{\mathrm{z}-1} (\Upsilon_{\mathrm{z}-\mathrm{j}-1}^{\alpha(r_{\mathrm{i}},\mathrm{t}_{\mathrm{z}})} - \Upsilon_{\mathrm{z}-\mathrm{j}}^{\alpha(r_{\mathrm{i}},\mathrm{t}_{\mathrm{z}})}) \bar{\zeta}^{\mathrm{j}} + \Upsilon_{\mathrm{z}-1}^{\alpha(r_{\mathrm{i}},\mathrm{t}_{\mathrm{z}})} \bar{\zeta}^{0} \right|, \tag{3.42}$$

$$\leq \frac{1}{(1+\mu(r_{\mathrm{i}},\mathrm{t}_{\mathrm{z}})\lambda_{\mathrm{i}})\,\Upsilon_0^{\alpha(r_{\mathrm{i}},\mathrm{t}_{\mathrm{z}})}} \left| \sum_{\mathrm{j}=1}^{\mathrm{z}-1} (\Upsilon_{\mathrm{z}-\mathrm{j}-1}^{\alpha(r_{\mathrm{i}},\mathrm{t}_{\mathrm{z}})} - \Upsilon_{\mathrm{z}-\mathrm{j}}^{\alpha(r_{\mathrm{i}},\mathrm{t}_{\mathrm{z}})}) \right| |\bar{\zeta}^{\mathrm{j}}| + \left| \Upsilon_{\mathrm{z}-1}^{\alpha(r_{\mathrm{i}},\mathrm{t}_{\mathrm{z}})} \right| |\bar{\zeta}^{0}|, \tag{3.43}$$

$$= \frac{1}{(1+\mu(r_{\mathrm{i}},\mathrm{t}_{\mathrm{z}})\lambda_{\mathrm{i}})\,\Upsilon_0^{\alpha(r_{\mathrm{i}},\mathrm{t}_{\mathrm{z}})}} \left| \sum_{\mathrm{j}=1}^{\mathrm{z}-1} (\Upsilon_{\mathrm{z}-\mathrm{j}-1}^{\alpha(r_{\mathrm{i}},\mathrm{t}_{\mathrm{z}})} - \Upsilon_{\mathrm{z}-\mathrm{j}}^{\alpha(r_{\mathrm{i}},\mathrm{t}_{\mathrm{z}})}) \right| |\bar{\zeta}^{0}| + \left| \Upsilon_{\mathrm{z}-1}^{\alpha(r_{\mathrm{i}},\mathrm{t}_{\mathrm{z}})} \right| |\bar{\zeta}^{0}|, \tag{3.44}$$

$$= \frac{1}{(1+\mu(r_{\mathrm{i}},\mathrm{t}_{\mathrm{z}})\lambda_{\mathrm{i}})\,\Upsilon_0^{\alpha(r_{\mathrm{i}},\mathrm{t}_{\mathrm{z}})}} |\bar{\zeta}^{0}|. \tag{3.45}$$

which means

$$|\bar{\zeta}^{\mathrm{z}}| \leq |\bar{\zeta}^{0}|, \ \mathrm{z} = 0, 1, \ldots, \mathbf{N}. \tag{3.46}$$

It is implied by the result (3.46)

$$\|\bar{\zeta}^{\mathrm{z}}\|_2 \leq \|\bar{\zeta}^{0}\|_0, \ \mathrm{z} = 0, 1, \ldots, \mathbf{N}. \tag{3.47}$$

Therefore, the numerical scheme is unconditionally stable. □

The algorithm for solving by the proposed numerical scheme (3.26) is given below.

Algorithm 2: Assessment of the VOTFSDE numerical solution (3.1)-(3.3)

Input: The domain $\mho = [0, \mathrm{L}] \times [0, \mathrm{T}]$, $\mathbf{M}$, $h = \mathrm{L}/\mathbf{M}$, $\mathbf{N}$, $\tau = \mathrm{T}/\mathbf{N}$, initial condition $\Phi(r)$, boundary conditions $\Psi_1(\mathtt{t})$, $\Psi_2(\mathtt{t})$ and $\alpha(r_{\mathtt{i}}, \mathtt{t}_{\mathtt{z}}) \in (0, 1)$

Output: The numerical solution at each discretization point $(r_{\mathtt{i}}, \mathtt{t}_{\mathtt{z}})$

for Numerical solution of VOTFSDE by difference scheme **do**

Step-1.1 Consider the step length in time and space variables

$\mathtt{t}_{\mathtt{z}} = \mathtt{z}\tau$, $\mathtt{z} = 0, 1, \ldots, \mathbf{N}$, $r_{\mathtt{i}} = \mathtt{i}h$, $\mathtt{i} = 0, 1, \ldots, \mathbf{M}$.

Step-1.2 Convert the problem (3.1)-(3.3) into the problem (3.10)-(3.11) by using the transformation (3.6)-(3.8).

Step-1.3 Apply L-123 approximation (3.14) to discretized the VOCD in time and the central difference scheme in spatial direction.

Step-1.4 Use the boundary conditions $\mathrm{u}(0, \mathtt{t}_{\mathtt{z}}) = \Psi_1(\mathtt{t}_{\mathtt{z}})$, and $\mathrm{u}(1, \mathtt{t}_{\mathtt{z}}) = \Psi_2(\mathtt{t}_{\mathtt{z}})$ to calculate the value of $\mathrm{u}_{\mathtt{i}}^{0}$ and $\mathrm{u}_{\mathbf{M}}^{\mathbf{N}}$, respectively.

Step-1.5 Calculate the numerical solution $\mathrm{u}_{\mathtt{i}}^{\mathtt{z}}$, $\mathtt{z} \geq 1$, by using the difference scheme (3.25).

Step-1.6 Repeat step (1.4) and (1.5) and use all the values of $\mathrm{u}_{\mathtt{i}}^{\mathtt{z}}$ at each previous time levels till we get the discrete solution of VOTFSDE at each discretised points $(r_{\mathtt{i}}, \mathtt{t}_{\mathtt{z}})$.

end

3.4 Numerical results and discussion

In this section, The accuracy of the proposed scheme for both cases is demonstrated by the following error norms

$$||\mathrm{u}-\mathrm{U}|| = \begin{cases} \left(\sum_{\mathsf{i}=1}^{N} h|\mathrm{u}(r_{\mathsf{i}},T)-\mathrm{U}(r_{\mathsf{i}},T)|^2\right)^{1/2}, & L_2Norm \\ max_{0\le \mathsf{i}\le N}|\mathrm{u}(r_{\mathsf{i}},T)-\mathrm{U}(r_{\mathsf{i}},T)|, & L_\infty Norm, \end{cases} \tag{3.48}$$

where $\mathrm{u}(r,\mathsf{t})$ and $\mathrm{U}(r,\mathsf{t})$ are exact and numerical solutions of the FDEs.

3.4.1 Numerical examples for the VOTFSDE

Example 3.1. Consider the variable-order time-fractional subdiffusion equation with homogeneous boundary conditions,

$${}_0\mathrm{D}_{\mathsf{t}}^{\alpha(r,\mathsf{t})}\mathrm{u}(r,\mathsf{t}) = \frac{\partial^2 \mathrm{u}(r,\mathsf{t})}{\partial x^2} + \mathsf{f}(r,\mathsf{t}), \quad (r,\mathsf{t}) \in [0,1]\times[0,1], \tag{3.49}$$

$$\mathrm{u}(r,0) = 10r^2(1-r), \quad 0 \le r \le 1, \tag{3.50}$$

$$\mathrm{u}(0,\mathsf{t}) = 0, \ \mathrm{u}(1,\mathsf{t}) = 0, \quad 0 \le \mathsf{t} \le 1. \tag{3.51}$$

with the source term

$$\mathsf{f}(r,\mathsf{t}) = 20r^2(1-r)\left[\frac{\mathsf{t}^{2-\alpha(r,\mathsf{t})}}{\Gamma(3-\alpha(r,\mathsf{t}))} + \frac{\mathsf{t}^{1-\alpha(r,\mathsf{t})}}{\Gamma(2-\alpha(r,\mathsf{t}))}\right] - 20(\mathsf{t}+1)^2(1-3r). \tag{3.52}$$

The exact solution of VOTFSDE in Ex. 3.1 is given by [35],

$$\mathrm{u}(r,\mathsf{t}) = 10r^2(1-r)(\mathsf{t}+1)^2. \tag{3.53}$$

The outcomes of Ex. 3.1 are as follows:

1. At time $\mathtt{t} = 1$, figure 3.1 is showing the maximum absolute error (Max. Abs. Error) for various $\alpha(r, \mathtt{t})$, when $(h, \tau) = (1/50, 1/32)$. In both the spatial and temporal directions, it can be seen that the Max. Abs. Error achieved accuracy upto 10^{-9} on a extremely small grid point. Up to third order is reached in the temporal order of convergence. (see Table 3.1).

2. At time $\mathtt{t} = 1$, figure 3.2 is showing the Max. Abs. Error at time for various $\alpha(r, \mathtt{t})$, when $h^2 = \tau$ i.e. $(h, \tau) = (1/16, 1/256)$. Here accuracy achieved upto 10^{-12}. Up to 6th order is reached in the spatial order of convergence. (see Table 3.2).

3. Table 3.3-3.4 compares the maximum error performance with the reduction in time and space grid size by scheme (3.26) and scheme given in [35].

4. Table 3.5 is showing the comparative study of maximum error at each spatial grid point. Figure 3.3 is showing the point wise Max. Abs. Error at time $\mathtt{t} = 1$ for $\alpha(r, \mathtt{t}) = \frac{1}{4}(2 + \sin(r\mathtt{t}))$, when $h^2 = \tau$ i.e. $(h, \tau) = (1/10, 1/100)$.

5. It can be observed from Tables 3.3-3.5 that the proposed scheme gives highly accurate results and convergence order than the existing scheme in [35].

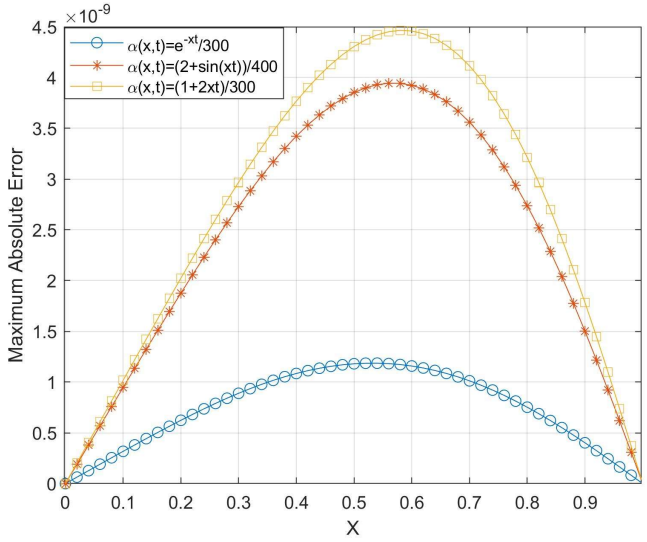

FIGURE 3.1: Max. Abs. Error of Ex. 3.1 for various $\alpha(r, \mathtt{t})$, $h = 1/50$, $\tau = 1/32$.

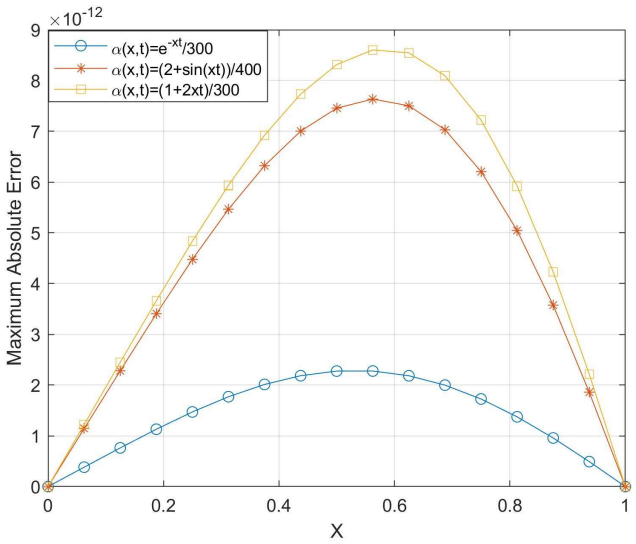

FIGURE 3.2: Max. Abs. Error of Ex. 3.1 for various $\alpha(r, \mathtt{t})$, $h^2 = \tau$.

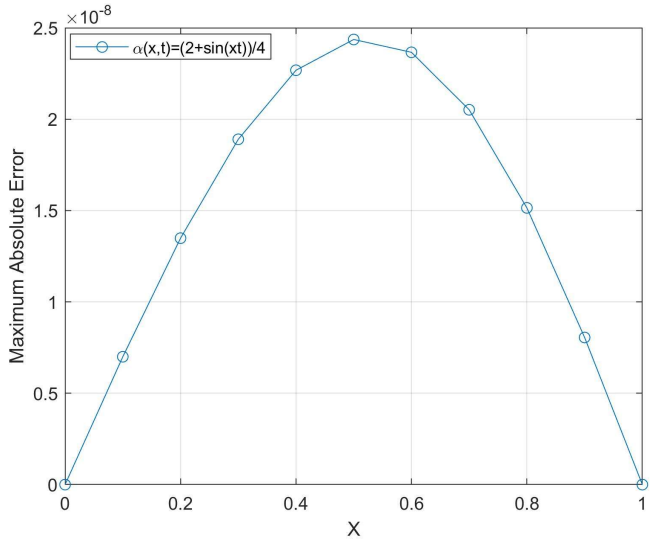

FIGURE 3.3: Point wise Max. Abs. Error of Ex. 3.1 for $\alpha(r,\mathtt{t}) = \dfrac{2+\sin(r\mathtt{t})}{4}$, $\tau = 1/100,\ h = 1/10$.

TABLE 3.1: At time $\mathtt{t} = 1$, L_2, L_∞ error of Ex. 3.1, when $h = 1/50$.

$\alpha(r,\mathtt{t})$	τ	Scheme (3.26)		Scheme (3.26)	
		L_2 Error	Order	L_∞ Error	Order
$\dfrac{e^{-r\mathtt{t}}}{300}$	1/4	4.819e-07	-	6.859e-07	-
	1/8	5.604e-08	3.104	7.977e-08	3.104
	1/16	6.776e-09	3.047	9.644e-09	3.048
	1/32	8.336e-10	3.023	1.186e-09	3.023
	1/64	1.034e-10	3.010	1.472e-10	3.010
$\dfrac{2+\sin(r\mathtt{t})}{400}$	1/4	1.597e-06	-	2.281e-06	-
	1/8	1.857e-07	3.104	2.652e-07	3.014
	1/16	2.245e-08	3.048	3.206e-08	3.048
	1/32	2.762e-09	3.023	3.945e-09	3.023
	1/64	3.425e-10	3.011	4.893e-10	3.011

$\alpha(r,\mathtt{t})$	τ	Scheme (3.26)		Scheme (3.26)	
		L_2 Error	Order	L_∞ Error	Order
$\frac{1+2r\mathtt{t}}{300}$	1/4	1.802e-06	-	2.584e-06	-
	1/8	2.095e-07	3.104	3.003e-07	3.104
	1/16	2.532e-08	3.048	3.630e-08	3.048
	1/32	3.115e-09	3.023	4.465e-09	3.023
	1/64	3.863e-10	3.011	5.538e-10	3.011

TABLE 3.2: At time $\mathtt{t} = 1$, L_2, L_∞ error of Ex. 3.1 for various $\alpha(r,\mathtt{t})$, when $h^2 = \tau$.

$\alpha(r,\mathtt{t})$	h	Scheme (3.26)		Scheme (3.26)	
		L_2 Error	Order	L_∞ Error	Order
$\frac{e^{-r\mathtt{t}}}{300}$	1/4	7.114e-09	-	1.008e-08	-
	1/8	1.046e-10	6.087	1.482e-10	6.088
	1/16	1.607e-12	6.025	2.277e-12	6.024
$\frac{2+\sin(r\mathtt{t})}{400}$	1/4	2.350e-08	-	3.266e-08	-
	1/8	3.466e-10	6.083	4.873e-10	6.066
	1/16	5.344e-12	6.019	7.636e-12	5.996
$\frac{1+2r\mathtt{t}}{300}$	1/4	2.647e-08	-	3.634e-08	-
	1/8	3.909e-10	6.081	5.560e-10	6.030
	1/16	6.016e-12	6.022	8.604e-12	6.014

TABLE 3.3: At time $\mathtt{t} = 1$, comparison of Max. Abs. Error for Ex. 3.1, when $h = 1/100$.

$\alpha(r,\mathtt{t})$	τ	In [35]		Scheme (3.26)	
		Maximum Error	Order	Maximum Error	Order
$\frac{2+\sin(r\mathtt{t})}{4}$	1/4	1.0408e-02	-	1.1863e-04	-
	1/8	4.1086e-03	1.34	2.4118e-05	2.2985
	1/16	1.1602e-03	1.36	3.4297e-06	2.8142
	1/32	6.1590e-04	1.38	5.0707e-07	2.7580

TABLE 3.4: At time $\mathtt{t} = 1$, comparison of Max. Abs. Error for Ex. 3.1, when $h^2 = \tau$.

$\alpha(r,\mathtt{t})$	h	In [35]		Scheme (3.26)	
		Maximum Error	Order	Maximum Error	Order
$\frac{2+\sin(r\mathtt{t})}{4}$	1/4	1.625e-03	-	3.7020e-06	-
	1/8	2.492e-04	2.70	8.0049e-08	5.53
	1/16	3.720e-05	2.74	2.0794e-09	5.26

TABLE 3.5: Numerical solution, exact solution, the pointwise Max. Abs. Error for $\alpha(r,\mathsf{t}) = \dfrac{2+\sin(r\mathsf{t})}{4}$, $\tau = 1/100$, $\mathsf{t} = 1$, $h = 1/10$.

r_i	In [35]			Scheme (3.26)	
	Numerical	Exact	Max. Abs. Error	Numerical	Max. Abs. Error
0.10	0.36002996	0.36000000	2.9960e-05	0.36000000	6.9981e-09
0.20	1.28005972	1.28000000	5.9720e-05	1.28000001	1.3487e-08
0.30	2.52008803	2.52000000	8.8030e-05	2.52000001	1.8899e-08
0.40	3.84011251	3.84000000	1.1251e-04	3.84000002	2.2678e-08
0.50	5.00012981	5.00000000	1.2981e-04	5.00000002	2.4368e-08
0.60	5.76013595	5.76000000	1.3595e-04	5.76000002	2.3659e-08
0.70	5.88012705	5.88000000	1.2705e-04	5.88000002	2.0514e-08
0.80	5.12010048	5.12000000	1.0048e-04	5.12000001	1.5144e-08
0.90	3.24005643	3.24000000	5.6430e-05	3.24000000	8.0524e-09

Example 3.2. Consider the VOTFSDE,

$$ {}_0\mathrm{D}_t^{\alpha(r,\mathsf{t})}\mathrm{u}(r,\mathsf{t}) = \frac{\partial^2 \mathrm{u}(r,\mathsf{t})}{\partial r^2} + \mathsf{f}(r,\mathsf{t}), \quad (r,\mathsf{t}) \in [0,1]\times[0,1], \tag{3.54} $$

$$ \mathrm{u}(r,0) = r(1-r), \quad 0 \le r \le 1, \tag{3.55} $$

$$ \mathrm{u}(0,\mathsf{t}) = 0, \ \mathrm{u}(1,\mathsf{t}) = 0, \quad 0 \le \mathsf{t} \le 1, \tag{3.56} $$

where the source term is

$$ \mathsf{f}(r,\mathsf{t}) = r(1-r)\frac{6t^{3-\alpha(r,\mathsf{t})}}{\Gamma(4-\alpha(r,\mathsf{t}))} + 2\mathsf{t}^3. \tag{3.57} $$

The exact solution is given by

$$ \mathrm{u}(r,\mathsf{t}) = r(1-r)\mathsf{t}^3. \tag{3.58} $$

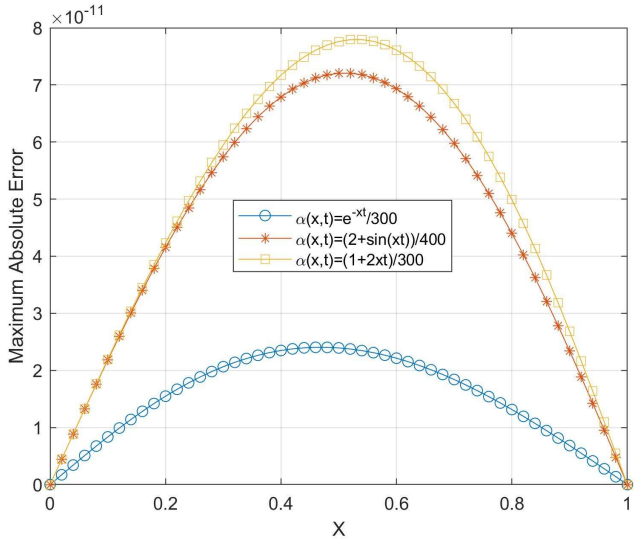

FIGURE 3.4: Max. Abs. Error of Ex. 3.2 for various $\alpha(r,\mathtt{t})$, $\tau = 1/32$, $h = 1/50$.

The outcomes of Ex. 3.2 are as follows:

1. At time $\mathtt{t} = 1$, figure 3.4 is showing the Max. Abs. Error for various $\alpha(r,\mathtt{t})$, when $(h,\tau) = (1/50, 1/32)$. It can be seen that the Max. Abs. Error achieved accuracy upto 10^{-11} on a extremely small grid point in both spatial and time direction. Up to 4th order is reached in the temporal order of convergence. (see Table 3.6).

2. At time $\mathtt{t} = 1$, figure 3.5 is showing the Max. Abs. Error for various $\alpha(r,\mathtt{t})$, when $h^2 = \tau$ i.e. $(h,\tau) = (1/16, 1/256)$. Here accuracy reaches upto 10^{-14}. Up to 8th order is reached in the spatial order of convergence. (see Table 3.7).

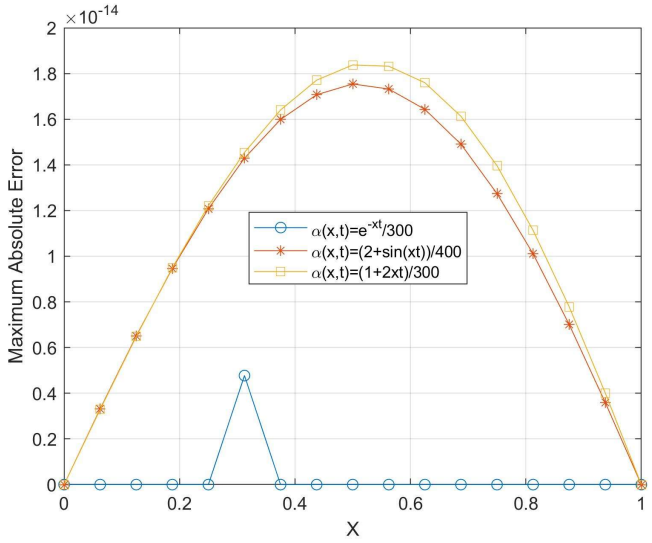

FIGURE 3.5: Max. Abs. Error of Ex. 3.2 for various $\alpha(r,\mathtt{t})$, $h^2=\tau$.

TABLE 3.6: At time $\mathtt{t}=1$, L_2, L_∞ errors of Ex. 3.2, when $h=1/50$.

$\alpha(r,\mathtt{t})$	τ	Scheme (3.26)		Scheme (3.26)	
		L_2 error	Order	L_∞ error	Order
$\frac{e^{-r\mathtt{t}}}{300}$	1/4	9.435e-08	-	1.330e-07	-
	1/8	4.880e-09	4.273	4.878e-09	4.273
	1/16	2.826e-10	4.110	3.983e-10	4.110
	1/32	1.706e-11	4.050	2.404e-11	4.050
	1/64	1.050e-12	4.021	1.480e-12	4.021
$\frac{2+\sin(r\mathtt{t})}{400}$	1/4	2.831e-07	-	3.988e-07	-
	1/8	1.464e-08	4.273	2.062e-08	4.273
	1/16	8.474e-10	4.110	1.194e-09	4.110
	1/32	5.115e-11	4.050	7.206e-11	4.050
	1/64	3.144e-12	4.024	4.429e-12	4.024
$\frac{1+2r\mathtt{t}}{300}$	1/4	3.056e-07	-	4.317e-07	-
	1/8	1.580e-08	4.274	2.231e-08	4.274
	1/16	9.142e-10	4.110	1.291e-09	4.110
	1/32	5.517e-11	4.050	7.793e-11	4.050
	1/64	3.391e-12	4.024	4.790e-12	4.024

TABLE 3.7: At time $\mathsf{t} = 1$, L_2, L_∞ errors of Ex. 3.2, when $h^2 = \tau$.

$\alpha(r,\mathsf{t})$	h	Scheme (3.26)		Scheme (3.26)	
		L_2 error	Order	L_∞ error	Order
$\frac{e^{-r\mathsf{t}}}{300}$	1/4	2.954e-10	-	4.136e-10	-
	1/8	1.061e-12	8.121	1.487e-12	8.119
	1/16	1.193e-15	9.795	4.774e-15	8.283
$\frac{2+\sin(r\mathsf{t})}{400}$	1/4	8.866e-10	-	1.247e-09	-
	1/8	3.180e-12	8.123	4.478e-12	8.121
	1/16	1.242e-14	8.000	1.754e-14	7.996
$\frac{1+2r\mathsf{t}}{300}$	1/4	9.566e-10	-	1.343e-09	-
	1/8	3.430e-12	8.123	4.822e-12	8.121
	1/16	1.305e-14	8.038	1.837e-14	8.035

Example 3.3. Conisder the VOTFSDE with non-homogeneous boundary conditions

$$\frac{\partial \mathsf{u}(r,\mathsf{t})}{\partial \mathsf{t}} = {}_0D_{\mathsf{t}}^{1-\alpha(r,\mathsf{t})}\frac{\partial^2 \mathsf{u}(r,\mathsf{t})}{\partial x^2} + \mathsf{f}(r,\mathsf{t}). \tag{3.59}$$

$$\mathsf{u}(r,0) = 0, \quad 0 \le r \le 1, \tag{3.60}$$

$$\mathsf{u}(0,\mathsf{t}) = \mathsf{t}^2, \ \mathsf{u}(1,\mathsf{t}) = e\mathsf{t}^2, \quad 0 \le \mathsf{t} \le 1 \tag{3.61}$$

and source term is

$$\mathsf{f}(r,\mathsf{t}) = 2e^r\left[\mathsf{t} - \frac{\mathsf{t}^{1+\alpha(r,\mathsf{t})}}{\Gamma(2+\alpha(r,\mathsf{t}))}\right] \tag{3.62}$$

The exact solution is [1]

$$\mathsf{u}(r,\mathsf{t}) = e^r\mathsf{t}^2. \tag{3.63}$$

The outcomes of Ex. 3.3 are:

1. Fig. 3.6, is showing Max. Abs. Error in Ex. 3.3 for various $\alpha(r,\mathtt{t})$. Table 3.8 gave the L_2 and L_∞ error and temporal order of convergence at extremely small grid points.

2. Table 3.7 gives the comparison of L_2 and L_∞ at $\mathtt{t}=1$ for various $\alpha(r,\mathtt{t})$ with the scheme given in [1] when $h=1/100$. It can be observed from this table that the scheme provide high accuracy as compared to the existing scheme.

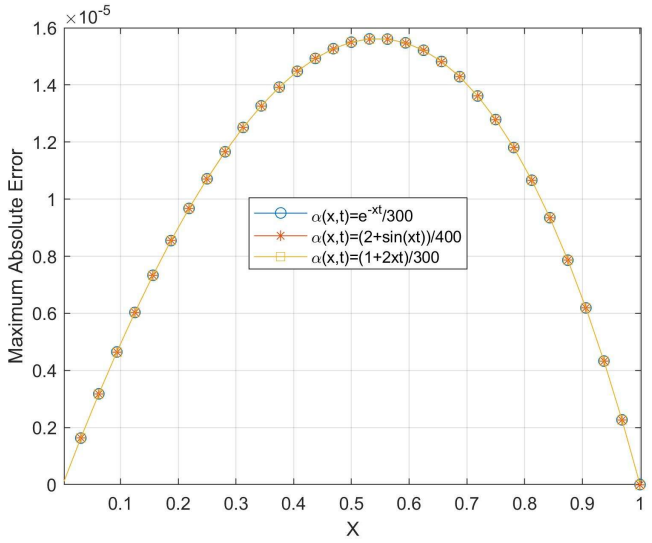

FIGURE 3.6: Max. Abs. Error of Ex. 3.3 for various $\alpha(r,\mathtt{t})$, $\tau=1/32$, $h=1/32$.

TABLE 3.8: At time $\mathtt{t} = 1$, L_2, L_∞ errors, order of convergence in time for Ex. 3.3.

$\alpha(r,\mathtt{t})$	(τ, h)	Scheme (3.26)		Scheme (3.26)	
		L_2 Error	Order	L_∞ Error	Order
$\frac{e^{-r\mathtt{t}}}{300}$	$\left(\frac{1}{4},\frac{1}{4}\right)$	7.238e-04	-	9.853e-04	-
	$\left(\frac{1}{8},\frac{1}{8}\right)$	1.823e-04	1.989	2.476e-04	1.992
	$\left(\frac{1}{16},\frac{1}{16}\right)$	4.565e-05	1.998	6.240e-05	1.988
	$\left(\frac{1}{32},\frac{1}{32}\right)$	1.141e-05	1.999	1.561e-05	1.999
$\frac{2+\sin(r\mathtt{t})}{400}$	$\left(\frac{1}{4},\frac{1}{4}\right)$	7.253e-04	-	9.873e-04	-
	$\left(\frac{1}{8},\frac{1}{8}\right)$	1.825e-04	1.990	2.478e-04	1.994
	$\left(\frac{1}{16},\frac{1}{16}\right)$	4.565e-05	1.998	6.242e-05	1.989
	$\left(\frac{1}{32},\frac{1}{32}\right)$	1.141e-05	2.000	1.561e-05	1.999
$\frac{1+2r\mathtt{t}}{300}$	$\left(\frac{1}{4},\frac{1}{4}\right)$	7.255e-04	-	9.876e-04	-
	$\left(\frac{1}{8},\frac{1}{8}\right)$	1.825e-04	1.991	2.478e-04	1.994
	$\left(\frac{1}{16},\frac{1}{16}\right)$	4.566e-05	1.999	6.242e-05	1.989
	$\left(\frac{1}{32},\frac{1}{32}\right)$	1.141e-05	2.000	1.561e-05	1.999

TABLE 3.9: Comparison of L_∞ and L_2 errors by scheme (3.26) and scheme given in [1] for Ex. 3.3.

$\alpha(r,\mathtt{t})$	τ	L_∞ error		L_2 error	
		In [1]	Scheme (3.26)	In [1]	Scheme (3.26)
$\frac{e^{-r\mathtt{t}}}{300}$	1/4	6.0309e-03	2.722e-06	4.4044e-02	1.994e-06
	1/8	1.5166e-03	1.730e-06	1.1078e-02	1.265e-06
	1/16	3.7704e-04	1.615e-06	2.7545e-03	1.180e-06
	1/32	9.3918e-05	1.602e-06	6.8622e-04	1.170e-06
$\frac{2+\sin(r\mathtt{t})}{400}$	1/4	6.0281e-03	5.213e-06	4.4023e-02	3.801e-06
	1/8	1.5171e-03	2.019e-06	1.1081e-02	1.474e-06
	1/16	3.7741e-04	1.650e-06	2.7572e-03	1.205e-06
	1/32	9.4057e-05	1.605e-06	6.8721e-04	1.173e-06
$\frac{1+2r\mathtt{t}}{300}$	1/4	6.0318e-03	5.657e-06	4.4051e-02	4.108e-06
	1/8	1.5182e-03	2.069e-06	1.1089e-02	1.510e-06
	1/16	3.7762e-04	1.656e-06	2.7587e-03	1.210e-06
	1/32	9.4079e-05	1.606e-06	6.8736e-04	1.173e-06

3.5 Conclusion

In this chapter, we have developed a higher order stable numerical approach for the variable-order time-fractional subdiffusion equation. For different values of the $\alpha(r,\mathtt{t})$, three numerical examples are used to validate the proposed scheme. The data reported in Table (3.1-3.9), as well as the numerical results shown in Figures (3.1-3.6), were found to be highly accurate with higher order of convergence. A comparison study with the present scheme is also provided in Table (3.3-3.5) and Table 3.9 to show the effectiveness and accuracy of the proposed scheme. For some numerical instances, this method provides

very high precision even with a relatively small number of grid points. The theoretical unconditional stability of the proposed numerical scheme is also discussed. The scheme is applicable to a wide range of other variable-order temporal fractional nonlinear problems.

****